JACS
JOURNAL OF THE AMERICAN CHEMICAL SOCIETY
Communication
pubs.acs.org/JACS

Tetragonal Phase of 6-Oxoverdazyl Bent-Core Derivatives with Photoinduced Ambipolar Charge Transport and Electrooptical Effects

Marcin Jasiński,[†] Damian Pociecha,[‡] Hirosato Monobe,[§] Jacek Szczytko,[∥] and Piotr Kaszyński*[,†,⊥]

[†]Faculty of Chemistry, University of Łódź, Tamka 12, 91403 Łódź, Poland
[‡]Department of Chemistry, University of Warsaw, 02-089 Warsaw, Poland
[§]Research Institute for Ubiquitous Energy Devices, National Institute of Advanced Industrial Science and Technology (AIST), Ikeda, Osaka 563-8577, Japan
[∥]Institute of Experimental Physics, Faculty of Physics, University of Warsaw, Hoża 69, 00-681 Warsaw, Poland
[⊥]Organic Materials Research Group, Department of Chemistry, Vanderbilt University, Nashville, Tennessee 37235, United States

Supporting Information

ABSTRACT: Bent-core mesogens containing 6-oxoverdazyl radical as the angular central unit exhibit rich polymorphism that includes isotropic−isotropic transition, re-entant isotropic (I_{re}), and a novel 3D tetragonal (*Tet*) phases. Surprisingly, the paramagnetic *Tet* phase interacts linearly with applied electric field and exhibits photoinduced ambipolar charge transport ($\mu \approx 10^{-3}$ cm^2 V^{-1} s^{-1}). Magnetic analysis showed gradual increase of antiferromagnetic interactions upon cooling.

There is increasing interest in bent-core mesogens due to their electrooptical switching and nonlinear optical (NLO) behavior[1,2] arising from a combination of polarity and diverse phase structures. The latter include a variety of lamellar and columnar phases,[3] which are typically formed by rod-like and disk-like molecules and are known to support hole transport[4−7] and some exhibit ambipolar charge transport.[8] Such materials are of interest for organic electronic[9−11] and solar cell[12−14] applications, which recently were also demonstrated for bent-core mesogens in a binary sytem with C_{60} derivatives.[15]

Stable radicals act as efficient organic semiconductors with a narrow electrochemical window[16] that facilitates charge pair photogeneration. In this context triphenylmethyl[17] and nitroxyl[18] discotic derivatives have been investigated, and we reported discotic behavior and photovoltaic properties of some verdazyl derivatives.[19,20] In continuation of our search for new types of supramolecular arrangements and enhanced charge transport, we focused on the bent-core molecular architecture with the verdazyl as the central unit. Here we demonstrate the verdazyl group as an angular element of the bent-core molecular structure and investigate thermal, electrooptical, magnetic, and photovoltaic properties of series **1**[**n**]−**3**[**n**].

Radicals in series **1**[**n**]−**3**[**n**] were obtained by esterification of diphenol **4** with appropriate acid chloride **5**[**n**]−**7**[**n**] (Scheme 1). The diphenol **4** was prepared in 84% yield by debenzylation of **8a**, which was obtained in 4 steps and 52% overall yield according to a method previously described for the 3-phenyl analogue.[21] An attempt to obtain **4** by basic hydrolysis of the analogous dibenzoyloxy derivative **8b** (X = OCOPh) failed and resulted in decomposition of the radical. Details are provided in the Supporting Information.

Scheme 1. Synthesis of Verdazyl Derivatives[a]

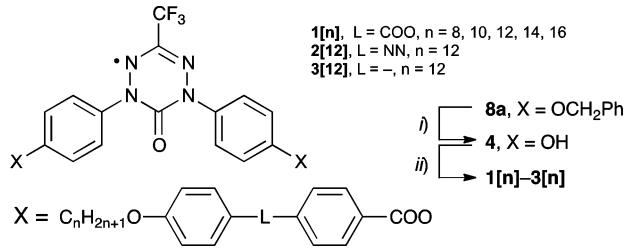

[a]Reagents and conditions: (*i*) H_2 (3 atm), Pd/C, THF-EtOH; (*ii*) RCOCl (**5**[**n**]−**7**[**n**]), DMAP, CH_2Cl_2, rt, 10 min.

Optical and thermal analyses demonstrated that all derivatives **1**[**n**]−**3**[**n**] exhibit mesogenic behavior (Table 1). Lower homologues in series **1**[**n**] exhibit nematic and a monotropic smectic (possibly SmA in **1**[**8**]; see Figures 1 and 2). However, higher homologues, **1**[**14**] and **1**[**16**], and also azo and biphenyl

Table 1. Thermal Properties of 1[n]−3[n][a]

	n	L	phase behavior
1	8	COO	Cr 150 (43.2) [Sm 141 (7.0)] N 197 (1.4) I
	10	COO	Cr 140 (41.1) N 174 (1.5) I
	12	COO	Cr 133 (79.3) [I_{re} 120][b,c] N 150 (0.8) I
	14	COO	Cr 98 (96.5) Tet 117 (6.0) I′ 128 (0.15)[d] I
	16	COO	Cr 84 (79.1) Tet 110 (3.4) I′ 124 (0.25)[d] I
2	12	NN	Cr 137 (22.4) Tet 142 (5.8) I′ 151 (0.17)[d] I
3	12		Cr 122 (15.8) Tet 129 (3.9) I′ 140 (0.17)[d] I

[a]Cr = crystal; N = nematic, Sm = smectic, Tet = tetragonal 3D; I and I′ = isotropic; enthalpy of transition in parentheses (kJ mol^{-1}). Recorded for fresh samples on heating. [b]Monotropic transition recorded on cooling. [c]Microscopic observation. See text. [d]ΔC_p (kJ mol^{-1} K^{-1}).

Received: July 25, 2014
Published: October 6, 2014

dx.doi.org/10.1021/ja507594h | J. Am. Chem. Soc. 2014, 136, 14658−14661

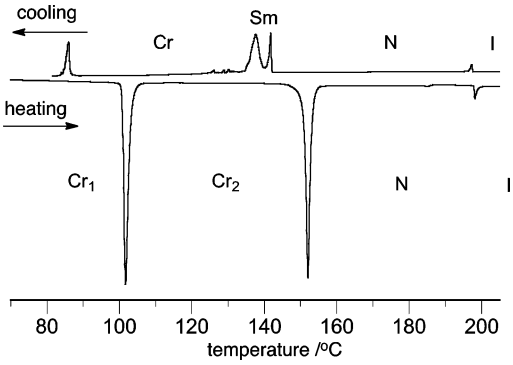

Figure 1. DSC trace of **1**[**8**]. The heating and cooling rates are 5 K min^{-1}.

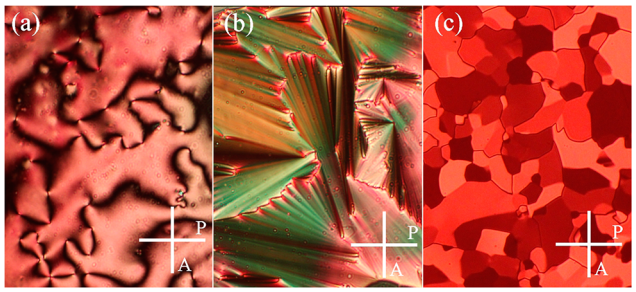

Figure 2. Optical textures of (a) N and (b) Sm phases in **1**[**8**] and (c) Tet phase in **1**[**16**].

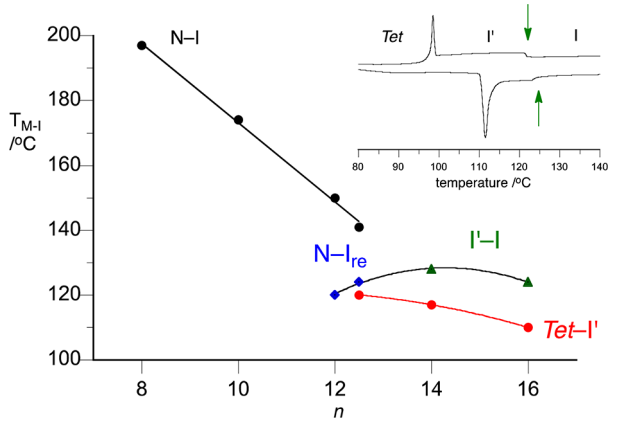

Figure 3. N–I (black), N–I_{re} (blue), Tet–I (red), and I′–I (green) phase transition temperatures as a function of the alkyl chain length in **1**[**n**]. The data point for **1**[**12.5**] was obtained from a mixture of **1**[**12**] and **1**[**14**]. Lines are guides for the eye. The inset shows a partial DSC trace for **1**[**16**] with marked I′–I transitions (lower curve heating; upper curve cooling).

derivatives, **2**[**12**] and **3**[**12**], exhibit a new three-dimensionally ordered (3D) tetragonal phase, Tet (*vide infra*), characterized by a mosaic texture (Figure 2c). Both T_{N-I} and $T_{Tet-I'}$ change monotonically in the homologous series of **1**[**n**] (Figure 3). A 3:1 mixture of **1**[**12**] and **1**[**14**], mimicking the **1**[**12.5**] homologue, exhibits both N and Tet phases separated by a monotropic re-entrant isotropic phase (I_{re}), also observed in quickly cooled samples of **1**[**12**]. This rare I_{re} phase has been reported for several other mesogens in which it separates nematic and cubic,[22] nematic and columnar,[23] smectic and columnar phases,[24,25] or two discotic phases.[26,27] More interestingly, all compounds exhibiting the Tet phase exhibit two adjacent optically isotropic phases. This is evident from reproducible thermal analyses, which show a second-order transition with a small hysteresis and $\Delta C_p \approx 0.2$ kJ K^{-1} mol^{-1} (Table 1 and inset in Figure 3; see also the Supporting Information) and coincides with a change in a slope of temperature dependence of positional correlation length observed by X-ray diffraction (XRD) for **1**[**16**] (see Figure S24 in the Supporting Information). Such an I′–I transition has been observed in other compounds typically forming 3D supramolecular structures, e.g., cubic, TGB, and blue phases.[28−30] Interestingly, the phase diagram (Figure 3) suggests that the appearance of both I_{re} and I′ phases in the homologous series could have similar origin.

Powder XRD analysis confirmed the liquid crystalline character of the Tet phase formed by **1**[**14**], **1**[**16**], **2**[**12**], and **3**[**12**]; a broad diffused signal centered at about 4.5 Å related to a short-range positional correlation of neighboring molecules was observed in the wide-angle region of the diffractograms (see Figure S22 in the Supporting Information). However, the small-angle region of the diffractograms exhibits a number of sharp, Bragg reflections, which can be fitted to a 3-dimensional tetragonal lattice[31] (Figure 4). Unfortunately, from the powder

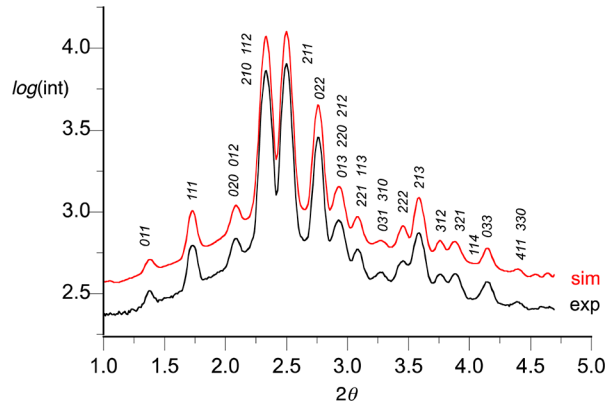

Figure 4. Small angle X-ray diffraction pattern for **1**[**14**] at 100 °C: experimental (black) and simulated (red) assuming a tetragonal crystallographic lattice with $P4_222$ symmetry, with unit cell parameters a = 84.6 Å and c = 97.5 Å.

XRD the exact symmetry of the lattice could not be determined. The highest symmetry that fits the experimental patterns of all compounds exhibiting the Tet phase is $P\bar{4}m2$. However, the observed ambipolar photoconduction in the Tet phase (*vide infra*) suggests a bicontinuous type structure and a space group $P4_222$, a subgroup of the $Pn\bar{3}m$ space group characteristic for one of the bicontinuous cubic LC phases, seems to be a better choice.

Liquid crystalline tetragonal phases have been previously observed as companions of bicontinuous cubic phases.[32] It should be also noted, that $P4_222$ symmetry has been considered for a tetragonal TGB phase.[33] The unit cell parameters of the Tet phase are about 10 nm for all compounds (Table 2), which corresponds to about two molecular lengths, and are essentially temperature independent.

Electrooptical experiments demonstrated that the tetragonal phase (Tet) reacts linearly with an applied field. The optical transmission of the sample follows the applied voltage and its direction, which suggests rotation of the optical axis rather than change in birefringence. Direct measurements of optical retardation and optical axis orientation confirmed that the sample birefringence is unaffected by the electric field, while the optical axis slightly rotates with the coefficient of 4.8(1) × 10^{-2}

dx.doi.org/10.1021/ja507594h | J. Am. Chem. Soc. 2014, 136, 14658−14661

Table 2. X-ray Diffraction Data for the Tet Phase of Selected Compounds

compd	temp (°C)	lattice parameters (Å)	number of molecules[a]
1[14]	100	a = 84.6, c = 97.5	340
1[16]	50	a = 92.0, c = 103.8	410
2[12]	120	a = 111.4, c = 76.8	505
3[12]	120	a = 84.4, c = 105.6	420

[a]Per unit cell, assuming density of 1.0 g cm^{-3}.

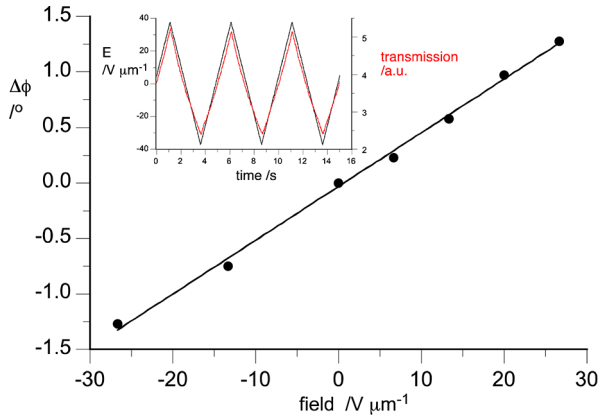

Figure 5. Change of optical axis orientation ($\Delta\phi$) as a function of applied electric field. The $\Delta\phi$ values are averaged for several domains of the Tet phase of **1**[16]. The inset shows optical transmission (red) in crossed-polarized setup upon application of triangular waveform voltage (black).

deg μm V^{-1}, as measured for **1**[16] (Figure 5). The observed linear change of the optical axis in the sample may suggest the existence of polar order in the tetragonal phase or a strong flexoelectric coupling. The effect is, however, smaller by an order of magnitude than that observed for a cholesteric phase.[34]

Magnetic studies at 7 T and temperature range of 2−400 K revealed paramagnetic behavior of **1**[16] in the liquid crystalline and isotropic phases with increasing antiferromagnetic interactions upon temperature lowering (Figure 6). Assuming ideal paramagnetic behavior in the isotropic phase, the diamagnetic correction was established using the Curie−Weiss law with θ = −19.6 K (see the Supporting Information). The effective magnetic moment (μ_{eff}) in the isotropic phase (400 K) is close to the value of 1.732 for an ideal paramagnet and corresponds to 99 ± 0.5% of spins (Figure 6). Upon cooling from 400 K, the μ_{eff} value continuously decreases without any abrupt changes.

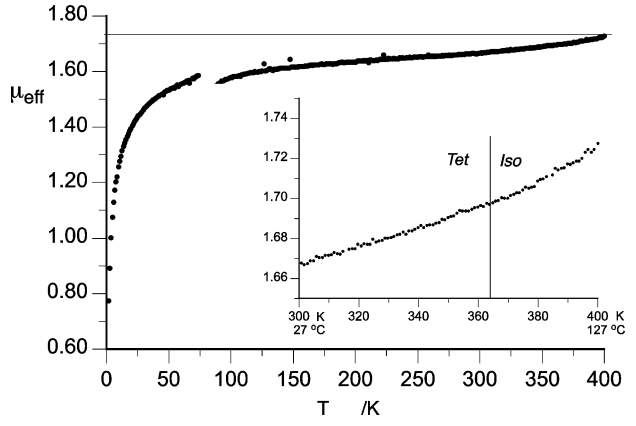

Figure 6. Effective magnetic moment, μ_{eff}, for **1**[16] vs temperature measured on cooling at 7 T (1 K min^{-1}). The horizontal line marks μ_{eff} = 1.732. The discontinuity around 75 K results from magnetization changing sign. The inset shows the expanded high temperature portion of the plot.

Time-of-flight (TOF) measurements found positive (hole) and negative (e^-) charge carrier mobilities (μ_h and μ_e) in an unaligned multidomain sample of **1**[16] to be nearly constant, 1 × 10^{-3} cm^2 V^{-1} s^{-1}, in a temperature range of 100 to 45 °C without electric field dependency. The measured mobility parameters fall in a typical range[4] of 10^{-4}−10^{-1} cm^2 V^{-1} s^{-1} and indicate microsegregation between the rigid molecular π cores and alkyl chains into channels in the Tet phase. The nearly constant values of mobility μ and consequently low activation energy (E_a = 0.03(1) eV) results presumably from a balance between the thermal activation of the charge hopping process and increasing molecular fluctuations with increasing temperature.[35] In the isotropic phase, the charge mobility was lower by a factor of 100.

For the first time we have demonstrated that 6-oxoverdazyl is an effective paramagnetic, polar angular element of bent-core mesogens. Its derivatives with three-ring substituents exhibit an unusual polymorphism, which includes 3D tetragonal, presumably bicontinuous phase and two distinct isotropic phases for longer terminal chains and smectic/nematic phases for lower homologues. Homologue **1**[12] shows a re-entrant isotropic phase below the nematic phase. The tetragonal phase exhibits ambipolar photoconduction with charge mobility $\mu \approx 1 \times 10^{-3}$ cm^2 V^{-1} s^{-1} and linear reorientation of optical axis under applied electric field. This raises an interesting possibility of coupling electrooptical and magnetic properties of the phase, with significant implications for development of new soft materials for molecular electronics and electrooptics.

Further experiments to explore this new class of paramagnetic polar materials and to understand the origin of the observed effects are under way.

■ ASSOCIATED CONTENT

Supporting Information

Full details of synthesis and characterization of compounds, NMR spectra, additional DSC, XRD, electrooptical, magnetization, and photovoltaic details and results. This material is available free of charge via the Internet at http://pubs.acs.org.

■ AUTHOR INFORMATION

Corresponding Author

*piotr.kaszynski@vanderbilt.edu

Notes

The authors declare no competing financial interest.

■ ACKNOWLEDGMENTS

Dedicated to Professor Josef Michl on the occasion of his 75th birthday.

This project was supported by the National Science Center (2011/01/B/ST5/06582, 2013/09/B/ST5/01230, and 2013/11/B/ST3/04193) and National Science Foundation (CHE-1214104) grants. M.J. thanks University of Łódź Foundation and Prof. S. Jankowski of Łódź University of Technology for help with hydrogenation experiments.

■ REFERENCES

(1) Etxebarria, J.; Ros, M. B. *J. Mater. Chem.* **2008**, *18*, 2919−2926.

(2) Iglesias, W.; Jákli, A. In *Hanbook of Liquid Crystals*; Goodby, J. W., Collings, P. J., Kato, T., Tschierske, C., Gleeson, H. F., Raynes, P., Eds.; Wiley-VCH: Mörlenbach, Germany, 2014; Vol. *8*, pp 799−817.
(3) Reddy, R. A.; Tschierske, C. *J. Mater. Chem.* **2006**, *16*, 907−961.
(4) Kaafarani, B. R. *Chem. Mater.* **2011**, *23*, 378−396.
(5) Pisula, W.; Kastler, M.; Wasserfallen, D.; Mondeshki, M.; Piris, J.; Schnell, I.; Müllen, K. *Chem. Mater.* **2006**, *18*, 3634−3640.
(6) Sergeyev, S.; Pisula, W.; Geerts, Y. H. *Chem. Soc. Rev.* **2007**, *36*, 1902−1929.
(7) Pisula, W.; Müllen, K. In *Hanbook of Liquid Crystals*; Goodby, J. W., Collings, P. J., Kato, T., Tschierske, C., Gleeson, H. F., Raynes, P., Eds.; Wiley-VCH: Mörlenbach, Germany, 2014; Vol. *8*, pp 627−673.
(8) Iino, H.; Hanna, J. *Opto-Electron. Rev.* **2005**, *13*, 295−302.
(9) Tsao, H. N.; Pisula, W.; Liu, Z.; Osikowicz, W.; Salaneck, W. R.; Müllen, K. *Adv. Mater.* **2008**, *20*, 2715−2719.
(10) Oikawa, K.; Monobe, H.; Nakayama, K.; Kimoto, T.; Tsuchiya, K.; Heinrich, B.; Guillon, D.; Shimizu, Y.; Yokoyama, M. *Adv. Mater.* **2007**, *19*, 1864−1868.
(11) Zhang, F.; Funahashi, M.; Tamaoki, N. *Org. Electron.* **2010**, *11*, 363−368.
(12) Schmidt-Mende, L.; Fechtenkötter, A.; Müllen, K.; Moons, E.; Friend, R. H.; MacKenzie, J. D. *Science* **2001**, *293*, 1119−1122.
(13) Schmidt-Mende, L.; Fechtenkötter, A.; Müllen, K.; Friend, R. H.; MacKenzie, J. D. *Physica* **2002**, *E14*, 263−267.
(14) van de Craats, A. M.; Warman, J. M.; Fechtenkötter, A.; Brand, J. D.; Harbison, M. A.; Müllen, K. *Adv. Mater.* **1999**, *11*, 1469−1472.
(15) Callahan, R. A.; Coffey, D. C.; Chen, D.; Clark, N. A.; Rumbles, G.; Walba, D. M. *ACS Appl. Mater. Interfaces* **2014**, *6*, 4823−4830.
(16) Hicks, R. G., Ed. *Stable Radicals: Fundamentals and Applied Aspects of Odd-Electron Compounds*; John Wiley & Sons: Chichester, U.K., 2010.
(17) Castellanos, S.; López-Calahorra, F.; Brillas, E.; Juliá, L.; Velasco, D. *Angew. Chem., Int. Ed.* **2009**, *48*, 6516−6519.
(18) Ravat, P.; Marszalek, T.; Pisula, W.; Müllen, K.; Baumgarten, M. *J. Am. Chem. Soc.* **2014**, *136*, 12860−12863.
(19) Jankowiak, A.; Pociecha, D.; Monobe, H.; Szczytko, J.; Kaszyński, P. *Chem. Commun.* **2012**, *48*, 7064−7066.
(20) Jankowiak, A.; Pociecha, D.; Szczytko, J.; Monobe, H.; Kaszyński, P. *J. Am. Chem. Soc.* **2012**, *134*, 2465−2468.
(21) Jasiński, M.; Gerding, J. S.; Jankowiak, A.; Gębicki, K.; Romański, J.; Jastrzębska, K.; Sivaramamoorthy, A.; Mason, K.; Evans, D. H.; Celeda, M.; Kaszyński, P. *J. Org. Chem.* **2013**, *78*, 7445−7454.
(22) Weissflog, W.; Letko, I.; Pelzl, G.; Diele, S. *Liq. Cryst.* **1995**, *18*, 867−870.
(23) Bilgin-Eran, B.; Tschierske, C.; Diele, S.; Baumeister, U. *J. Mater. Chem.* **2006**, *16*, 1145−1153.
(24) Pietrasik, U.; Szydłowska, J.; Krówczyński, A.; Pociecha, D.; Górecka, E.; Guillon, D. *J. Am. Chem. Soc.* **2002**, *124*, 8884−8890.
(25) Głębowska, A.; Przybylski, P.; Winek, M.; Krzyczkowska, P.; Krówczyński, A.; Szydłowska, J.; Pociecha, D.; Górecka, E. *J. Mater. Chem.* **2009**, *19*, 1395−1398.
(26) Warmerdam, T.; Frenkel, D.; Zijlstra, R. J. J. *Liq. Cryst.* **1988**, *3*, 149−152.
(27) Warmerdam, T. W.; Nolte, R. J. M.; Drenth, W.; van Miltenburg, J. C.; Frenkel, D.; Zijlstra, R. J. J. *Liq. Cryst.* **1988**, *3*, 1087−1104.
(28) Vogrin, M.; Vaupotič, N.; Wojcik, M. M.; Mieczkowski, J.; Madrak, K.; Pociecha, D.; Gorecka, E. *Phys. Chem. Chem. Phys.* **2014**, *16*, 16067−16074.
(29) Nishiyama, I.; Yamamoto, J.; Goodby, J. W.; Yokoyama, H. *Mol. Cryst. Liq. Cryst.* **2007**, *443*, 25−41.
(30) Nishiyama, I.; Yamamoto, J.; Goodby, J. W.; Yokoyama, H. *Liq. Cryst.* **2002**, *29*, 1409−1423.
(31) Three-dimensional phases of cubic symmetry have been rarely observed for bent-core materials, see Reddy, R. A.; Baumeister, U.; Keith, C.; Hahn, H.; Lang, H.; Tschierske, C. *Soft Matter* **2007**, *3*, 558−570. (b) Kang, S.; Harada, M.; Li, X.; Tokita, M.; Watanabe, J. *Soft Matter* **2012**, *8*, 1916−1922.
(32) Levelut, A.-M.; Clerc, M. *Liq. Cryst.* **1998**, *24*, 105−115.
(33) Levelut, A.-M.; Hallouin, E.; Bennemann, D.; Heppke, G.; Lötzsch, D. *J. Phys. II* **1997**, *7*, 981−1000.
(34) Patel, J. S.; Meyer, R. B. *Phys. Rev. Lett.* **1987**, *58*, 1538−1540.
(35) Funahashi, M.; Hanna, J.-I. *Adv. Mater.* **2005**, *17*, 594−598.